Role of the Bering Strait on the hysteresis of the ocean conveyor belt circulation and glacial climate stability

Aixue Hu[a,1], Gerald A. Meehl[a], Weiqing Han[b], Axel Timmermann[c], Bette Otto-Bliesner[a], Zhengyu Liu[d], Warren M. Washington[a], William Large[a], Ayako Abe-Ouchi[e], Masahide Kimoto[e], Kurt Lambeck[f], and Bingyi Wu[g]

[a]Climate and Global Dynamics Division, National Center for Atmospheric Research, Boulder, CO 80305; [b]Department of Atmospheric and Oceanic Sciences, University of Colorado, Boulder, CO 80301; [c]Department of Oceanography, University of Hawaii, HI 96822; [d]Center for Climate Research, Nelson Institute for Environmental Studies, University of Wisconsin, Madison, Wisconsin 53706; [e]Atmosphere and Ocean Research Institute, University of Tokyo, Chiba 277-8568, Japan; [f]Research School of Earth Sciences, The Australian National University, Canberra, ACT 0200, Australia; and [g]Chinese Academy of Meteorological Sciences, Beijing, China 100081

Edited by Isaac M. Held, Geophysical Fluid Dynamics Laboratory/NOAA, Princeton, NJ, and approved March 8, 2012 (received for review September 28, 2011)

Abrupt climate transitions, known as Dansgaard-Oeschger and Heinrich events, occurred frequently during the last glacial period, specifically from 80–11 thousand years before present, but were nearly absent during interglacial periods and the early stages of glacial periods, when major ice-sheets were still forming. Here we show, with a fully coupled state-of-the-art climate model, that closing the Bering Strait and preventing its throughflow between the Pacific and Arctic Oceans during the glacial period can lead to the emergence of stronger hysteresis behavior of the ocean conveyor belt circulation to create conditions that are conducive to triggering abrupt climate transitions. Hence, it is argued that even for greenhouse warming, abrupt climate transitions similar to those in the last glacial time are unlikely to occur as the Bering Strait remains open.

abrupt climate transitions | Atlantic Meridional Overturning Circulation

Abrupt climate transitions, known as Dansgaard-Oeschger (D/O) cycles, are a prominent feature of the last glacial period. Identified in different paleo-climate archives, such as Greenland ice cores (1–3), they occurred mostly from about 80–11 thousand years before present (kyr BP) (Fig. 1*A*). Layers of ice-rafted debris found in North Atlantic sediment cores provide further evidence for a different kind of climate instability, often associated with surging ice-sheets (4, 5). While it is still debated as to whether these variations in North Atlantic climate are driven externally—e.g. by solar forcing or originating from internal climate instabilities (6–10)—it has been established that the Atlantic Meridional Overturning Circulation (AMOC, or the ocean conveyor belt circulation) is at least involved (11–13). It also remains an open question why D/O events were absent during the Holocene and the beginning of the last glacial period, and more importantly whether this type of abrupt climate transition could occur in a future warmer climate associated with elevated atmospheric greenhouse gases.

The AMOC characterizes the zonally averaged oceanic circulation in the Atlantic which transports warm saltier upper ocean water from the rest of the oceans to the subpolar North Atlantic where this water loses heat to the atmosphere, becomes dense and sinks to depth, then flows southward and upwells elsewhere. Theoretical studies show that as freshwater forcing increases very slowly in the North Atlantic, the AMOC initially weakens slowly, and then suddenly collapses (ref. 14, Fig. 2*A*, black line). As freshwater forcing is subsequently slowly reduced, AMOC stays in the "off" mode until a critical value of freshwater forcing is attained that triggers a rapid AMOC resumption (Fig. 2*A*, red line). The abrupt transitions of the AMOC from "on" to "off," or vice versa, could induce significant cooling or warming events in the North Atlantic and surrounding regions by disrupting or enhancing the northward ocean heat transport in the Atlantic basin. Therefore, this AMOC hysteresis behavior has been used as a plausible mechanism to explain the abrupt climate transitions recorded in the Greenland Ice core record and supported by paleo-proxy observations (1–5, 11–13).

Studies based on earth system models of intermediate complexity (EMICs) and a coarse resolution atmosphere-ocean global climate model (AOGCM) indicate that the AMOC may exhibit multiple-equilibrium states under the same climatic forcing (15, 16), which supports a theoretical study (14). However, to date, there is no state-of-the-art AOGCM that supports the notion of a bistable ocean circulation under modern conditions with an open Bering Strait (BS), casting doubt on whether the AMOC mechanism could explain past abrupt climate transitions (17).

The stability of the glacial AMOC depends crucially on the salinity transport into the North Atlantic, which is partly controlled by the influx of fresher North Pacific surface waters into the Arctic Ocean via the BS (18–21). Presently this influx amounts to about 800-thousand-cubic-meters per second (0.8 Sv; 1 Sv $\equiv 10^6$ $m^3 s^{-1}$, ref. 22). Reconstructed past sea level changes (23) and Greenland ice core records (1–3) indicate that abrupt climate transitions occurred when the sea level was about 50 m below its present level (Fig. 1 *A* and *B*). With a present-day depth of about 50 m, BS was a land-bridge for most of the last glacial period, which allowed for early human migration to North America. More accurately computed relative sea level changes in the BS (see *Supporting Information*) suggest that the North Pacific was closed off from the Arctic Ocean from about 80–11 kyr B.P (Fig. 1*C*), which roughly coincides with the time of strong D/O and millennial-scale variability. Earlier studies speculated that the BS may have played a major role in the occurrence of these abrupt climate transitions through controlling the AMOC's response to external freshwater forcing (18–21). Furthermore, in subsequent modeling studies it was demonstrated that a BS closure is likely to have affected the stability of the major Laurentide ice-sheet (24), consistent with a recent marine core study (25).

Model and Experiments

Here we evaluate the potential impact of the BS closure/opening on the glacial climate stability by testing the role of the Bering Strait on AMOC hysteresis. A fully coupled state-of-the-art

Author contributions: A.H. designed research; A.H. performed research; K.L. contributed new reagents/analytic tools; A.H., G.A.M., W.H., A.T., B.O.-B., Z.L., W.M.W., W.L., A.A.-O., M.K., K.L., and B.W. analyzed data; and A.H., G.A.M., W.H., A.T., B.O.-B., Z.L., W.M.W., W.L., A.A.-O., M.K., K.L., and B.W. wrote the paper.

The authors declare no conflict of interest.

This article is a PNAS Direct Submission.

[1]To whom correspondence should be addressed. E-mail: ahu@ucar.edu.

This article contains supporting information online at www.pnas.org/lookup/suppl/doi:10.1073/pnas.1116014109/-/DCSupplemental.

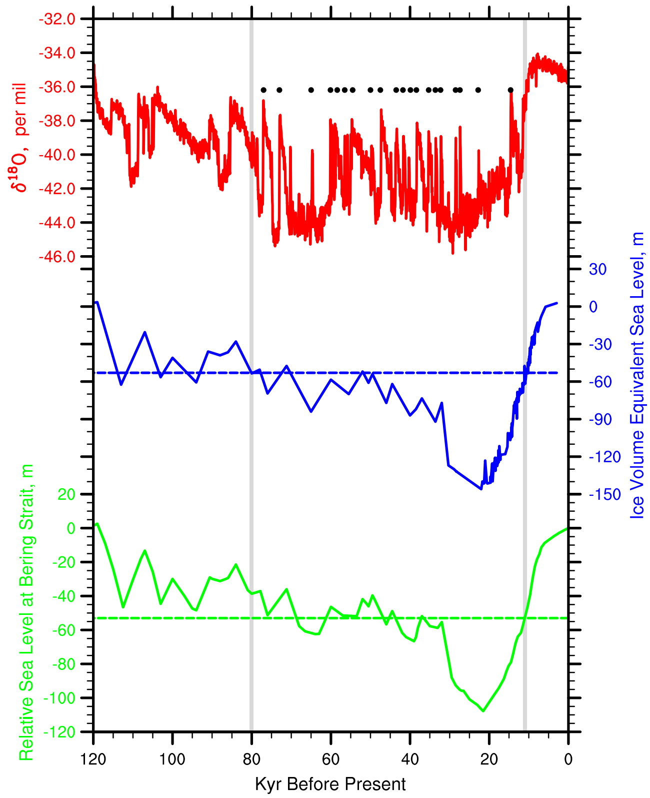

Fig. 1. Time series of the North Greenland Ice core δO^{18} record (*A*, ref. 1), ice-volume equivalent sea level (*B*, ref. 21) and the predicted relative sea level in the BS region (*C*). The dashed lines indicate the present-day depth of the Bering Strait. All sea levels are relative to the present-day sea level. The dots indicate Dansgaard-Oeschger events (2, 3).

AOGCM—the Community Climate System Model, version 3 (CCSM3, ref. 26)— is employed with a resolution high enough to properly simulate effects of BS closure on the North Atlantic climate system and its stability. This model simulates realistic BS transports under present-day conditions (18) in comparison to observations (22). To isolate the potential effect of the BS closure/opening on the AMOC hysteresis, two identical water-hosing simulations under present-day boundary conditions are carried out, except that the BS is open in one (Open Bering Strait, or OBS) but closed in the other (Closed Bering Strait, or CBS).

Following ref. 15, an initial freshwater flux of 200 m^3/s (about 4 times the value used in ref. 15) is added to the North Atlantic between 20 and 50 °N. This freshwater flux increases by 200 m^3/s per year until the AMOC collapses. Afterwards this additional freshwater forcing linearly decreases to zero at the same rate. With such a slow rate change, a freshwater forcing increment/decrement of 0.1 Sv takes place over 500 y, thus maintaining the AMOC at a quasiequilibrium state throughout our simulation. Therefore, our simulations differ significantly from many previous coupled model studies (18, 19) since here we focus specifically on the BS impact on the AMOC hysteresis, not AMOC's response to a short-lived freshwater pulse. Our simulations also stand out from EMIC type simulations (15) by using an AOGCM with a reasonably high horizontal resolution that captures atmosphere-ocean-sea-ice coupling more realistically.

Results

In the OBS simulation, the AMOC (defined as the maximum of the Atlantic meridional overturning streamfunction below 500 m depth) slows down almost linearly as the freshwater forcing increases until AMOC collapses (Fig. 2*B*, Fig. S1*A*). As the freshwater forcing is reduced, AMOC stays in the off mode only for a short period (less than 400 yr) before it starts to linearly strengthen. This seems to confirm previous results which indicate that, with an open BS, the AMOC off mode is an advectively unstable mode (19, 27). Therefore, with an open BS, there are no AMOC multiple equilibria. When BS is closed, however, the AMOC exhibits a behavior reminiscent of the hysteresis behavior in the simplified models (15): AMOC weakens slowly as freshwater forcing increases initially, with a significant acceleration when freshwater forcing exceeds 0.3 Sv, leading to an AMOC collapse for a freshwater forcing of 0.42 Sv. After that, the AMOC stays near the off mode for about 1,400 yr while the freshwater forcing gradually reduces, before it finally returns to the prehosing level when the freshwater forcing drops below 0.15 Sv (Fig. S1*A*). The AMOC recovery from off to active mode is, however, not as sharp as indicated in theoretical studies (14) and intermediate complexity models (15, 28), perhaps due to the damping associated with local and remote air-sea interactions. Additionally, the AMOC system might not be completely in equilibrium at each point on the curve, creating possible transients.

As the AMOC collapses, the mean surface temperatures of Greenland drop by 12 °C in both simulations (Fig. 2*C*, Fig. S1*B*), comparable to the magnitude of Greenland temperature variations in the abrupt climate change events recorded in the Greenland ice core data (29), confirming that an AMOC collapse could indeed induce large temperature changes in Greenland.

Although the AMOC recovers more abruptly in the CBS simulation than in the OBS simulation, the increase of Greenland temperatures is actually not as abrupt in the former as in the latter simulation. As suggested by Fig. 2*D* and Fig. S1*C*, the Greenland temperature change seems closely associated with the alterations of the Atlantic meridional heat transport (MHT) at 65 °N, which is closely related to the strength of North Atlantic deep convection. This deep convection restarts about 600 yr earlier in the Nordic Seas than in the Labrador and Irminger Seas in the CBS simulation (Fig. 3), resulting in a two-stage recovery of the Atlantic deep convection and a slower increase of Greenland temperature. In contrast, deep convection in these two regions in the OBS simulation restarts less than 300 yr apart, leading to a more abrupt Greenland warming. This two-stage recovery in the CBS simulation may be an artifact of the modern-day background climate used in this experiment. Under glacial conditions, the Nordic Seas were mostly sea ice covered and deep convection possibly occurred mostly in the Labrador and Irminger Seas. This might have led to a one-stage recovery of the Atlantic deep convection, resulting in a more abrupt warming in Greenland, such as in ref. 17.

The different AMOC responses to freshwater forcing in our simulations can be attributed to variations of the BS throughflow. Earlier studies indicate that with an open BS, the flow through this strait is controlled primarily by the sea level difference between the Pacific and the Arctic (Atlantic), with a higher sea level in the former (19, 30). In the OBS experiment, a fresher North Atlantic and a weaker AMOC lead to a dynamic sea level rise in the North Atlantic (31–33). This reduces, or even reverses, the sea level contrast between the Pacific and the Atlantic, leading to a weakened/reversed BS throughflow (Fig. 4*A*, Fig. S2, Fig. 3*A*), resulting in a reduced freshwater transport from the Pacific into the North Atlantic, and even transporting the now fresher North Atlantic water back into the North Pacific. In any case, this process reduces the freshwater flux into the North Atlantic from across the Arctic. There is subsequently less freshwater convergence and a smaller salinity anomaly in the North Atlantic (Fig. 4*A*, Fig. S3*A*), and this prevents a sudden AMOC collapse. When the freshwater forcing gradually reduces after the AMOC collapses eventually, the freshwater anomaly in the Atlantic still is diverging out of the subpolar region into the South Atlantic and North Pacific via surface ocean currents with the same speed as when AMOC has just collapsed. This will make the surface ocean saltier, leading to a weakened oceanic stratification, a restart of

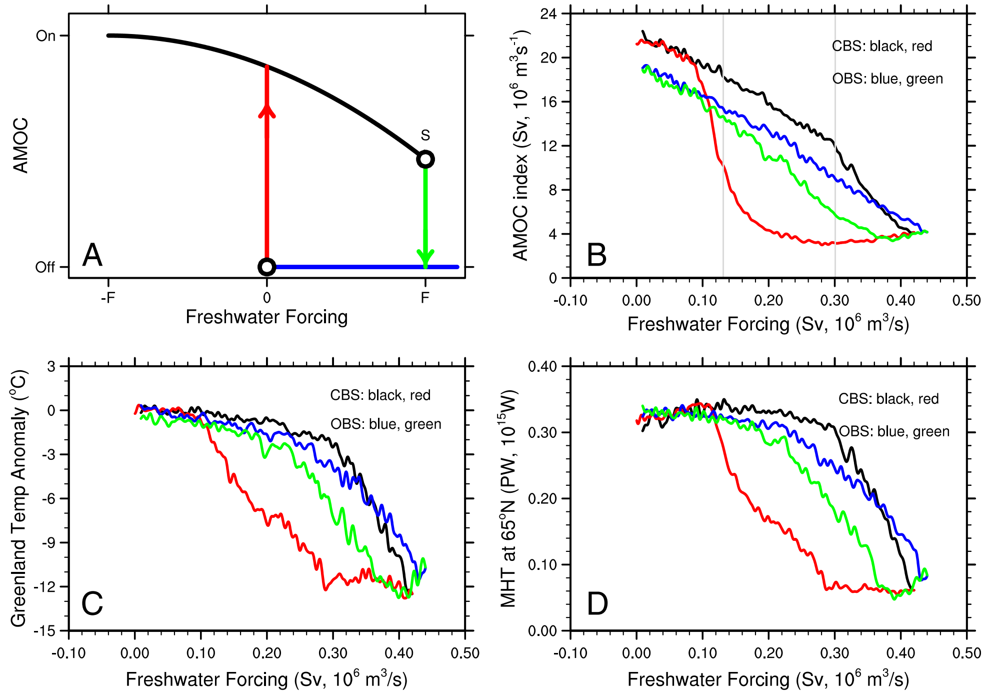

Fig. 2. Theoretical and simulated AMOC hysteresis curves (*A*, *B*) and the associated changes of Greenland surface temperature and meridional heat transport at 65 °N in the Atlantic (*C*, *D*). In panel a), "S" is the bifurcation point beyond which AMOC collapses and the "$+/-$F" values indicate the freshwater forcing strength. In (*B*), (*C*), and (*D*), the black/red (blue/green) lines are for the closed (open) BS simulation. The black/blue (red/green) lines represent the phase of freshwater forcing increase (decrease) in these simulations. Note that a change of the freshwater forcing by 0.1 Sv (Sv $\equiv 10^6$ m^3 s^{-1}) in this figure takes place over 500 model years.

deep convection and the AMOC (Fig. 3, Fig. S4), and a resumption of fresh Pacific water being transported into the North Atlantic via the BS (Fig. S2), thus preventing the AMOC from a sudden jump in strength (19). Instead it increases slowly in magnitude.

With a closed BS, as freshwater forcing strengthens in the North Atlantic, the AMOC also weakens and part of the freshwater added to the North Atlantic is transported into the Arctic. However, the closed BS prevents this freshwater from being

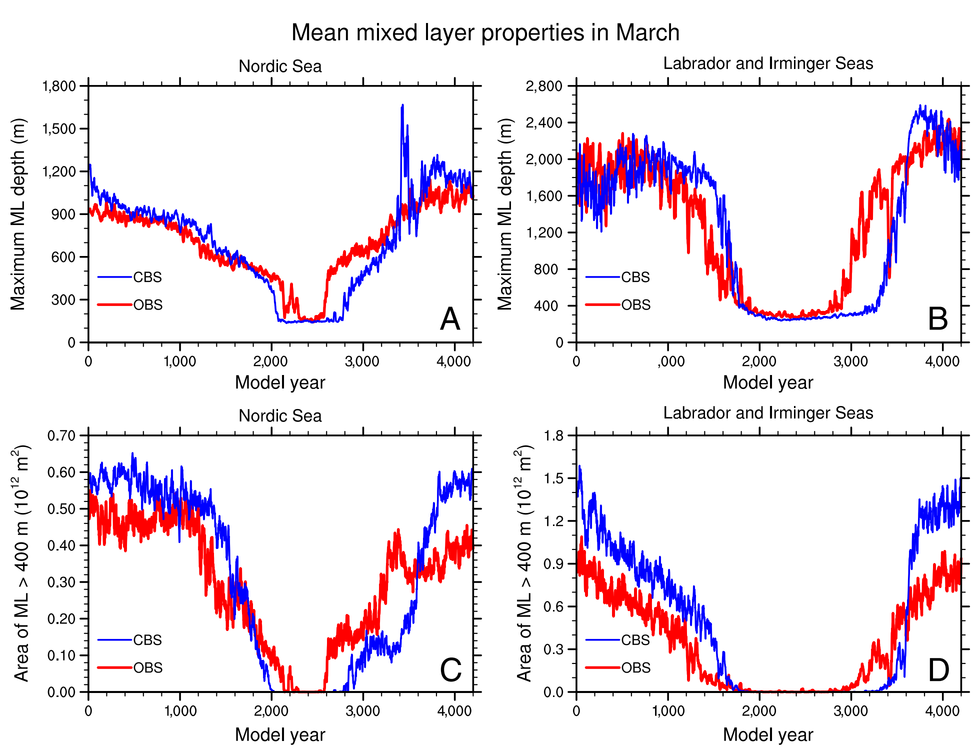

Fig. 3. Changes of the maximum March mixed layer depth and the area over which the maximum March mixed layer depth is greater than 400 meters in the Nordic Sea (*A*, *C*), and the Labrador and Irminger Seas (*B*, *D*). Blue lines are for the closed Bering Strait simulation and red lines for the open Bering Strait simulation.

carried into the Pacific, inducing a prominent freshening effect in the Arctic and a sea level rise, especially along the edges of the Arctic. As a result, a large surface cyclonic gyre forms in the subpolar North Atlantic and the Arctic basins (Fig. 4*B*, Fig. S3*B*). This subpolar-Arctic cyclonic gyre transports the Arctic freshwater anomaly back into the North Atlantic, generating an enhanced freshwater convergence there and a much greater negative surface salinity anomaly (Fig. 4*B*). This reduces the upper ocean water density (Fig. S4), strengthens the upper ocean stratification, and suppresses deep convection in the subpolar North Atlantic, leading to the collapse of the AMOC in this simulation. Once the AMOC collapses, the ocean's ability to transport the North Atlantic freshwater anomaly elsewhere of the world ocean through the overturning circulation is greatly reduced. Therefore, the divergence of this North Atlantic freshwater anomaly depends mostly on the much less efficient water mass exchange between the subpolar-Arctic cyclonic gyre and the subtropical gyre. As the freshwater forcing in the North Atlantic starts to weaken, the resulting freshwater anomaly in the North Atlantic (Fig. S4) can only be transported southward because of the closed BS, thus delaying the removal of the freshwater anomaly and leading to a delayed recovery of the AMOC (19). Once the Arctic freshwater anomaly becomes sufficiently small due to the transport by the oceanic currents and the atmospheric circulation, this big subpolar-Arctic cyclonic gyre breaks into two gyres again—a cyclonic gyre in the subpolar North Atlantic and an anticyclonic gyre in the Arctic, reducing the freshwater convergence in the subpolar North Atlantic, leading to renewal of the deep convection there (Fig. S4) and a rapid AMOC recovery on timescales of a few hundred years.

The effect of the BS closure on the AMOC and the adjustment of the global scale ocean circulation can be further illustrated from the zonal mean salinity and meridional overturning streamfunction fields in the Atlantic and Pacific basins during the weak AMOC phase (Fig. 5) and strong AMOC phase (Fig. S5). Resulting from the changes of the BS transport in the OBS simulation, the upper few hundred meters of the North Atlantic are much saltier in the OBS run than in the CBS run. But the upper North Pacific is much fresher in the OBS run than in the CBS run due to the reduced/reversed freshwater transport from the North Pacific into North Atlantic via the BS (see Fig. 4). Resulting from these different salinity distributions in the two basins, although the Atlantic overturning patterns are quite similar in these two simulations when AMOC is off (Fig. 5), the Pacific overturning circulations are quite different. As illustrate in ref. 34 and Fig. S6, a Pacific MOC sets up in the CBS simulation due to this saltier North Pacific, but not in the OBS simulation. On the other hand, the fresher upper North Atlantic in the CBS simulation prevents a quick resumption of deep convection, thus keeping the AMOC in the off mode for much longer, even in case of weakened external freshwater forcing. These processes lead to the AMOC hysteresis in the CBS simulation. The surge of freshwater from the North Atlantic into the North Pacific via the BS and into the southern oceans in the OBS simulation leads to an early resumption of the deep convection in the North Atlantic (19), preventing the occurrence of the AMOC hysteresis in the OBS simulation.

Conclusion and Discussion

Our AOGCM simulations have suggested that under present-day conditions, a strong AMOC hysteresis can only be found when the BS is closed. With an open BS, the AMOC does not exhibit an apparent hysteresis from the freshwater forcing. These results imply that if the AMOC hysteresis is indeed a plausible mechanism to explain past abrupt climate transitions, such as the D/O events, these abrupt climate transitions could occur only during glacial times with a (nearly) closed BS. With an open BS, such as during the Holocene and in the future warmer climate associated with elevated levels of atmospheric greenhouse gases, our results indicate that the manifestations of bistability are unlikely to occur, reducing the chances for abrupt climate transitions associated with an AMOC collapse or recovery.

Our results also suggest that the discharge of land-based ice (or the instability of the land-based ice, ref. 35) might be only one of the necessary conditions to induce abrupt climate transitions, with the existence of the AMOC hysteresis being another one. For example, due to the lack of AMOC hysteresis, although the discharged land-based ice volume during the early Holocene is equivalent to about a 50 m global sea level rise, there have been no abrupt climate transitions in this period of similar magnitude to

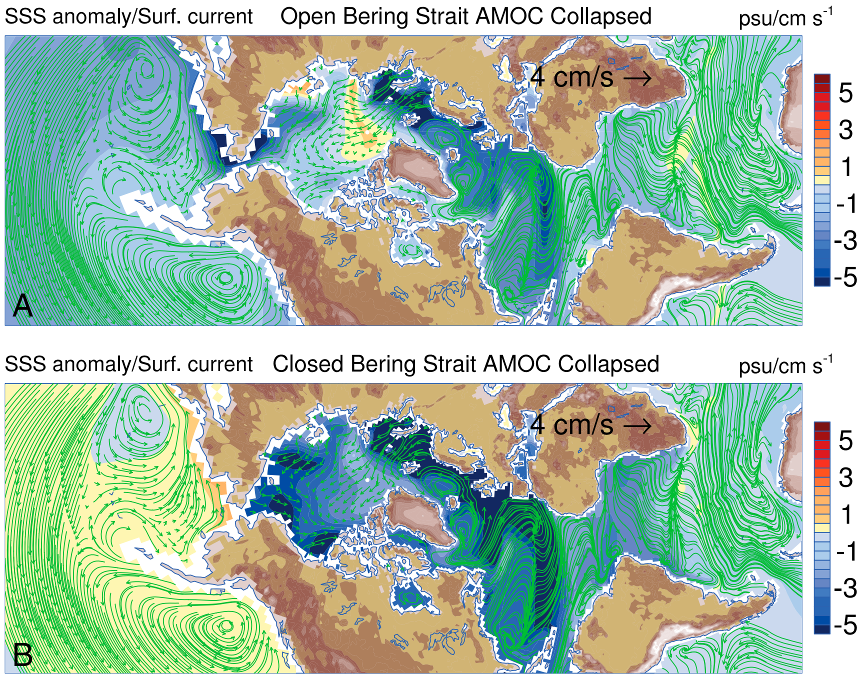

Fig. 4. Sea surface salinity (SSS) anomaly and sea surface currents when AMOC collapses for the open Bering Strait (*A*) and closed Bering Strait (*B*) simulations. The arrows are the sea surface currents with units of cm/s. The shading is the SSS anomaly with a contour interval of 0.5 psu.

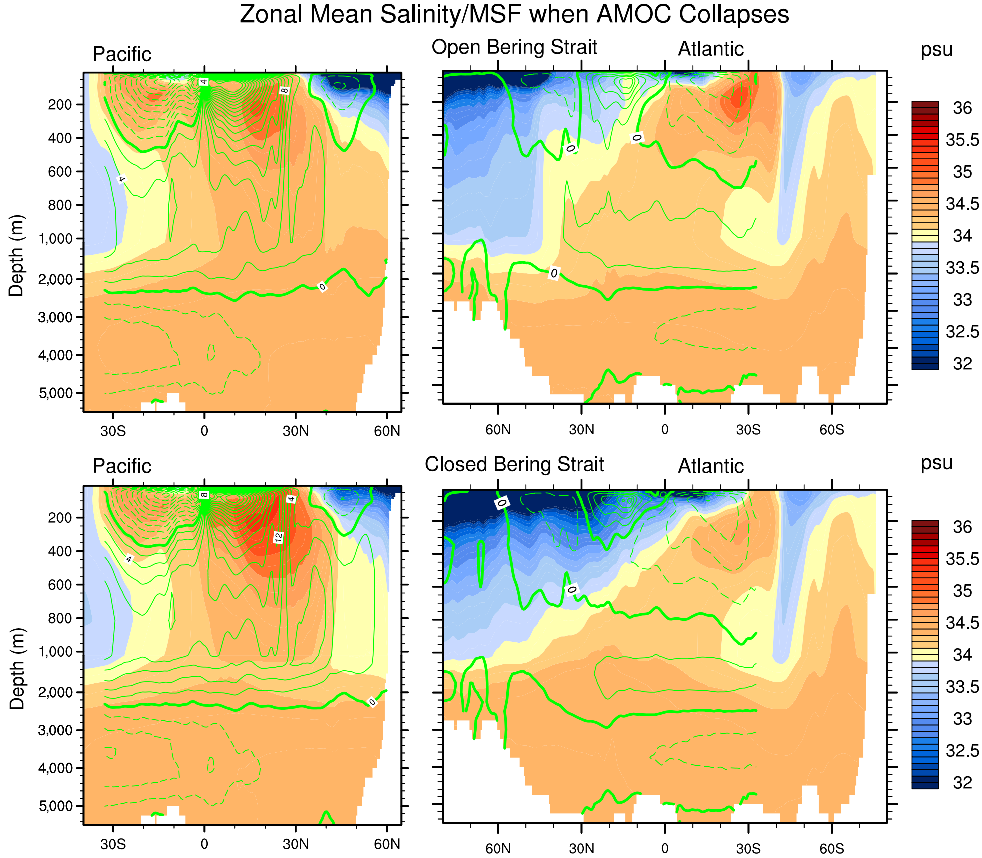

Fig. 5. Zonal mean salinity (shading) and meridional streamfunction (contour) in the Pacific (*Left*) and the Atlantic (*Right*) with a collapsed AMOC. The contour interval of the meridional streamfunction is 2 Sv, and that of zonal mean salinity is 0.1 psu. The upper panels are for the open Bering Strait simulation and lower panels for the closed Bering Strait simulation. Note: the scale for the upper 1,000 m of the ocean is stretched.

those that occurred during the last glacial period. Moreover, although the same conclusion regarding abrupt climate transitions only being able to occur during glacial times has been reached, the mechanism for glacial climate instability proposed in this study is fundamentally different from the mechanism proposed by a previous study (21) in which the authors proposed only that a BS closure has prevented the freshwater anomaly from being exported into the North Pacific. The lack of the AMOC hysteresis with an open Bering Strait could be the key for the absence of the abrupt climate change events during the early Holocene while major discharge of continental ice was still ongoing (Fig. 1*B*).

In order to isolate the BS effects on AMOC hysteresis and with the concern of possible future abrupt climate changes in mind, we intentionally used the same climate boundary condition—the present-day condition. Questions may be raised regarding whether our result with a closed BS would hold if glacial boundary conditions had been used. Earlier AOGCM studies showed that the AMOC's response to a strong pulse of freshwater forcing in the North Atlantic under present-day and glacial conditions is similar with a closed Bering Strait (19), suggesting that the conclusions reached here would be valid for glacial times. However, some previous simple model studies on AMOC hysteresis show diversified results under these climate conditions. Some indicate that AMOC hysteresis exists under both last glacial maximum (LGM) and present-day conditions, but with a narrower AMOC hysteresis width in the former than in the latter (36–38). Others suggest that under LGM conditions, the AMOC only has one stable mode (28). Moreover, due to the crudeness of these simple models, the BS cannot be represented properly and normally it is closed. Thus the results from this type of model are mostly equivalent to our closed BS simulation (more discussion in *Supporting Information*). Therefore, although our model could not simulate all of the physical processes in the Atlantic basin perfectly, the underlying physical mechanism we explore here is plausible to explain the questions we raised at the beginning. Thus we conclude it is very likely that the results reached here would hold under glacial conditions, at least qualitatively. However further study using glacial climate boundary conditions and multimodels is still needed for a further understanding of past abrupt climate transitions.

ACKNOWLEDGMENTS. A portion of this study was supported by the Office of Science (BER), U.S. Department of Energy, Cooperative Agreement No. DE-FC02-97ER62402. The National Center for Atmospheric Research is sponsored by the National Science Foundation. This research used resources of the National Energy Research Scientific Computing Center, which is supported by the Office of Science of the U.S. Department of Energy under Contract DE-AC02-05CH11231. Weiqing Han is supported by National Science Foundation CAREER award OCE 0847605 and NASA OSTST award NNX08AR62G.

1. North Greenland Ice Core Project members (2004) High-resolution record of Northern Hemisphere climate extending into the last interglacial period. *Nature* 431:147–151.
2. Dansgaard W, et al. (1993) Evidence for general instability for past climate from a 250-kyr ice-core record. *Nature* 364:218–220.
3. Ditlevsen P-D, Kristensen M-S, Andersen K-K (2005) The recurrence time of Dansgaard-Oeschger events and limits on the possible periodic component. *J Climate* 18:2594–2603.
4. Heinrich H (1988) Origin and consequences of cyclic ice rafting in the northeast Atlantic Ocean during the past 130,000 years. *Quat Res* 29:142–152.
5. Hemming S-R (2004) Heinrich events: Massive late Pleistocene detritus layers of the North Atlantic and their global climate imprint. *Rev Geophys* 42:RG1005, doi:10.1029/2003RG000128.
6. Braun H, et al. (2005) Possible solar origin of the 1470-year glacial climate cycle demonstrated in a coupled model. *Nature* 438:208–211.

7. Schulz M (2002) On the 1470-year pacing of Dansgaard-Oeschger warm events. *Paleoceanography* 17:1014, doi: 10.1029/2000PA000571.
8. Alley R-B, MacAyeal D-R (1994) Ice-rafted debris associated with bing/purge oscillations of the Laurentide ice sheet. *Paleoceanography* 9:503–511.
9. Broecker W-S (1994) Massive iceberg discharges as triggers for global climate change. *Nature* 372:421–424.
10. Dima M, Lohmann G (2009) Conceptual model for millennial climate variability: a possible combined solar-thermohaline circulation origin for the ∼1,500-year cycle. *Climate Dynamics* 32:301–311.
11. Clark P-U, et al. (2007) *Ocean Circulation: Mechanisms and Impacts*, eds A Schmittner, J Chiang, and S Hemming (American Geophysical Union, Washington, DC.), Geophysical Monograph, 173, pp pp209–246.
12. Gutjahr M, Hoogakker B, Frank M, McCave I (2010) Changes in North Atlantic Deep Water strength and bottom water masses during Marine Isotope Stage 3 (45–35 ka BP). *Quaternary Sci Rev* 29:2451–2461.
13. Zahn R, et al. (1997) Thermohaline instability in the North Atlantic during meltwater events: Stable isotope and ice-rafted detritus records from core SO75-26KL, Portuguese margin. *Paleoceanography* 12:696–710.
14. Rahmstorf S (1995) Bifurcations of the Atlantic Thermohaline circulation in response to changes in the hydrological cycle. *Nature* 378:145–149.
15. Rahmstorf S, et al. (2005) Thermohaline circulation hysteresis: A model intercomparison. *Geophys Res Lett* 32:L23605, doi: 10.1029/2005GL023655.
16. Hawkins , et al. (2011) Bistability of the Atlantic overturning circulation in a global climate model and links to ocean freshwater transport. *Geophys Res Lett* 38: L10605, doi: 10.1029/2011GL047208.
17. Liu Z, et al. (2009) Transient simulation of last deglaciation with a new mechanism for Bolling-Allerod warming. *Science* 325:310–314.
18. Hu A, Meehl G-A, Han W (2007) Role of the Bering Strait in the thermohaline circulation and abrupt climate change. *Geophys Res Lett* 34:L05704, doi: 10.1029/2006GL028906.
19. Hu A, et al. (2008) Response of thermohaline circulation to freshwater forcing under present day and LGM conditions. *J Climate* 21:2239–2258.
20. De Boer A-M, Nof D (2004) The exhaust valve of the North Atlantic. *J Climate* 17:417–422.
21. De Bore A-M, Nof D (2004) The Bering Strait's grip on the northern hemisphere climate. *Deep-Sea Res Pt I* 51:1347–1366.
22. Woodgate R-A, Aagaard K (2005) Revising the Bering Strait freshwater flux into the Arctic Ocean. *Geophys Res Lett* 32:L02602, doi: 10.1029/2004GL021747.
23. Lambeck K, Chappell J (2001) Sea level change through the last glacial cycle. *Science* 292:679–686.
24. Hu A, et al. (2010) Influence of Bering Strait flow and North Atlantic circulation on glacial sea level changes. *Nat Geosci* 3:118–121, doi: 10.1038/NGEO729.
25. Grützner J, Higgins S-M (2010) Threshold behaviour of millennial scale variability in deep water hydrography inferred from a 1.1 Ma long record of sediment provenace at the southern Gardar Drift. *Paleoceanography* 25:PA4204, doi: 10.1029/2009PA001873.
26. Collins W-D, et al. (2006) The Community Climate System Model: CCSM3. *J Climate* 19:2122–2143.
27. Ganopolski A, Rahmstorf S (2001) Rapid changes of glacial climate simulated in a coupled climate model. *Nature* 409:153–158.
28. Krebs U, Timmermann A (2007) Fast advective recovery of the Atlantic meridional overturning circulation after a Heinrich event. *Paleoceanography* 22:PA1220, doi: 10.1029/2005PA001259.
29. Alley R-B, et al. (2003) Abrupt climate change. *Science* 299:2005–2010.
30. Shaffer G, Bendtsen J (1994) Role of the Bering Strait in controlling North Atlantic Ocean circulation and climate. *Nature* 367:354–357.
31. Levermann A, et al. (2005) Dynamic sea level changes following changes in the thermohaline circulation. *Clim Dynam* 24:347–354.
32. Yin J, Schlesinger M-E, Stouffer R-J (2009) Model projections of rapid sea level rise on the mortheast coast of the United States. *Nat Geosci* 2:262–266, doi: 10.1038/NGEO462.
33. Hu A, Meehl G-A, Han W, Yin J (2009) Transient response of the MOC and climate to potential melting of the Greenland Ice Sheet in the 21st century. *Geophys Res Lett* 36: L10707, doi: 10.1029/2009GL037998.
34. Hu A, et al. (2012) The Pacific-Atlantic seesaw and the Bering Strait. *Geophys Res Lett* 38:L03702, doi: 10.1029/2011GL050567.
35. Schulz M, Berger W-H, Sarnthein M, Grootes P-M (1999) Amplitude variations of 1470-year climate oscillations during the last 100,000 years linked to fluctuations of continental ice mass. *Geophys Res Lett* 26:3385–3388.
36. Prange M, Romanova V, Lohmann G (2002) The glacial Thermohaline circulation: stable or unstable? *Geophys Res Lett* 29, doi: 10.1029/2002GL015337.
37. Weber S-L, Drijfhout S-S (2007) Stability of the Atlantic meridional overturning circulation in the last glacial maximum climate. *Geophys Res Lett* 34:L22706, doi: 10.1029/2007GL031437.
38. Paillard D (2001) Glacial hiccups. *Nature* 409:147–148.

Supporting Information

Hu et al. 10.1073/pnas.1116014109

SI Text

SI Models and Experiments. ***a. Model.*** The state-of-the-art coupled climate model used in this study is the National Center for Atmospheric Research (NCAR) Community Climate System Model version 3 (CCSM3, ref. 1) which has been developed by NCAR scientists, in collaboration with Department of Energy research laboratories, and university scientists. The atmospheric component in the version of CCSM3 employed here is the Community Atmospheric Model version 3 (CAM3) using spectral dynamics at T42 resolution (grid points roughly every 240 km) and 26 hybrid levels vertically. The ocean model is a version of the Parallel Ocean Program (POP) developed at Los Alamos National Lab with 1° horizontal resolution and enhanced meridional resolution (1/3°) in the equatorial tropics and the North Atlantic and with 40 vertical levels (2). The sea ice model is the Community Sea Ice Model version 5 (CSIM5) with elastic-viscous-plastic dynamics, a subgrid-scale thickness distribution, and energy conserving thermodynamics. The land model is the Community Land Model version 3 (CLM3).

The ocean model of CCSM3 is a level-coordinate model based on POP 1.4 (3). The model solves the primitive equations in a generalized orthogonal coordinate in the horizontal using the hydrostatic and Boussinesq approximations. A linearized, implicit free-surface formulation is used to solve the barotropic equation, which requires the first-level thickness not to be too thin. Because the freshwater fluxes are treated as virtual salt fluxes relative to the global mean salinity, the integrated global ocean volume does not change in POP. The ocean model has 320 (zonal) X 384 (meridional) grid points horizontally and 40 levels in vertical (Fig. S7). The ocean domain is global, including Hudson Bay, the Mediterranean Sea, and the Persian Gulf. The Bering Strait and Northwest passage are open to the Arctic Ocean in standard CCSM3 model. The model grid is in spherical coordinates in the Southern Hemisphere, but the North Pole is displaced into Greenland at 80 °N and 40 °W in the Northern Hemisphere. In the Southern Hemisphere, the ocean model resolution is uniform at 1.125° in the zonal direction, but it varies significantly in the meridional direction, with the finest meridional resolution at the equator (0.27°), and monotonically increases to about 0.53° at 32°S, then keeps constant farther south (0.53°). Due to the displaced North Pole, the model resolution becomes much finer in the North Atlantic, and a bit coarser in the North Pacific (Fig. S7). The vertical resolution monotonically increases from 10 to 250 m from the surface to a depth of about 2,000 m, below which the resolution keeps uniformly at 250 m. The minimum ocean depth is 30 m and the maximum is 5,500 m. (The ocean model layer thickness from top to bottom (unit: meter): 10, 10.1,10.3,10.6,11, 11.7, 12.4 13.4, 14.6, 16.7, 18.2, 20.8, 24.1, 28.6, 34.7, 43.2, 55.2, 72.3, 96.7, 130, 170, 208, 233.6, 245.3, 249, 250, 250, 250, 250, 250, 250, 250, 250, 250, 250, 250, 250, 250, 250, 250.).

In the model tracer equations, the Gent and McWilliams (4) isopycnal transport parameterization with a mixing coefficient of 600 $m^2 s^{-1}$ is used. The vertical mixing coefficients are determined by the KPP scheme (5). In the ocean interior, the background internal wave mixing diffusivity varies in the vertical from 0.1×10^{-4} $m^2 s^{-1}$ near the surface to 1.0×10^{-4} $m^2 s^{-1}$ in the abyssal ocean.

There are three grid points in the narrowest place of the Bering Strait with a depth of 30, 50, and 50 meters in the standard CCSM3 ocean component. The width of the Bering Strait is about 170 km, which is slightly wider than the Bering Strait in reality which is about 150 km. In our closed Bering Strait simulation, these three grid points are changed to land points.

b. General model performance in simulating present-day climate. The CCSM3 model performance has been documented by a series papers in a special issue of Journal of Climate which was published in 2006. Here we will give a short summary of the overall performance of the CCSM3 in simulating the present-day climate.

In the T85 version of the CCSM3, the atmospheric energy balance at the top of the atmosphere and at the earth surface are very close to the observations, and are improved significantly in comparison to the previous version of the CCSM model—CCSM2 (1). The sea surface temperature biases are significantly improved too. The mean bias in CCSM3 relative to the HadISST is only 0.03 °C, with a root mean square error of 1.53 °C. The sea ice distribution agrees reasonably well with the satellite-based observations, and the in situ thickness observations. The CCSM3's equilibrium climate sensitivity due to doubling of the atmospheric CO_2 is 2.7 °C, and the transient climate response is 1.5 °C. In the control simulation, which is run under constant solar and greenhouse gas forcing, the globally averaged surface air temperature trend is only about −0.011 °C century^{-1} (6). The mean strength of the Atlantic Meridional Overturning circulation (AMOC) is about 21.9 Sv, comparable to observation-based estimates (e.g., ref. 7).

The simulated flow patterns in the Pacific-Arctic-North Atlantic in the control runs are shown in SF3. In the open Bering Strait control simulation, the fresher Pacific water flows into the Arctic through the Bering Strait, then this water flows anticyclonicly in the Arctic, then exits the Arctic via Fram Strait. Afterward this water flows along the east Greenland coast, exits the Denmark Strait, loops around the southern tip of the Greenland, and turns north toward the west Greenland coast, joining the Labrador Sea gyre. This feature of the simulated flow pattern is similar to that suggested from observations (8). In the closed Bering Strait simulation, the basic flow pattern in these regions is similar to that in the open Bering Strait simulation. However, due to the absence of Bering Strait throughflow, the surface currents in the Arctic are much weaker, and the exchange of water mass between the Arctic and the North Atlantic is also weaker in this closed Bering Strait simulation.

In CCSM3, the model horizontal resolution can affect the strength of the AMOC. As shown in ref. 9, the mean AMOC is stronger in the high resolution version (T85 atmosphere and 1 degree ocean) of the CCSM3 than in the low resolution version (T31 atmosphere and 3 degree ocean). The response of the AMOC to doubling CO_2 is larger in terms of percentage change in the low resolution CCSM3 than in the high resolution CCSM3. Previous studies on the AMOC's response to freshwater forcing added to different regions in the Atlantic-Arctic region show that the AMOC is not really sensitive to where the freshwater forcing is added to the Atlantic. As long as the freshwater forcing is strong enough, the AMOC will collapse under last glacial maximum conditions (10, 11). Therefore, the horizontal resolution of the model does affect the AMOC's mean state and its response to external forcings in CCSM3 quantitatively, but not qualitatively. For example, in response to CO_2 forcing the AMOC weakens in all versions of the CCSM3.

c. Experiment design. In this study, we did two experiments with everything identical except one has an open Bering Strait (OBS) and the other has a closed Bering Strait (CBS). Following

Rahmstorf et al. (12), the additional freshwater forcing is added into the North Atlantic between 20 and 50 °N with an initial value of 200 m^3/s. This freshwater forcing increases linearly every year with an amount of 200 m^3/s until the Atlantic meridional overturning circulation (AMOC) shuts down. Then this additional freshwater forcing linearly decreases 200 m^3/s per year until the additional freshwater forcing becomes zero. This initial additional freshwater flux is very small and the rate of increment/decrement later on is also very slow (it takes 500 model years for the added freshwater forcing to increase by 0.1 Sv [$\mathrm{Sv} \equiv 10^6\ \mathrm{m}^3\,\mathrm{s}^{-1}$, or one million cubic meters per second]). Thus these should be sufficient to keep the AMOC in a quasiequilibrium state throughout our simulation. The climate boundary condition used in these simulations is present-day.

In the open Bering Strait simulation, the AMOC collapses after 2,200 years with a peak freshwater forcing of 0.44 Sv. In the closed Bering Strait simulation, the AMOC collapses after 2,100 years with a peak freshwater forcing of 0.42 Sv. In this latter experiment, the AMOC restarts at about year 3,400, with a freshwater forcing of 0.14 Sv. Thus in our closed Bering Strait simulation, the interval of freshwater forcing for an AMOC from active to collapse is 0.28 Sv, similar to that shown in Rahmstorf et al. (12).

The simulations discussed here were carried out at National Energy Research Scientific Computing Center (NERSC) at Lawrence Berkeley National Laboratory. The model simulations run about 15 model years in one calendar day, and one whole simulation took about a year and half to finish.

d. Justification for the use of the present-day climate boundary conditions. In our open and closed Bering Strait simulations, the present-day climate boundary conditions are used. Since this is our first attempt to isolate the effect of the Bering Strait opening/closure on AMOC hysteresis, and either present-day or glacial background climate could not fit both of our twin experiments, we decided to use the present-day background climate. This is because of concern about possible abrupt climate transitions due to a sudden collapse of the AMOC in a future warmer climate. For example, the present-day background climate will not fit the closed Bering Strait simulation, but a glacial condition will not really fit the open Bering Strait simulation either. Here what we want to examine is if the AMOC hysteresis is a plausible mechanism to explain past abrupt climate transitions during glacial time, and why these abrupt climate transitions did not occur during the Holocene, even though the freshwater runoff from the melting ice sheet was still huge, especially during the first half of the Holocene. More importantly, if significant mass loss from the Greenland and Antarctic ice sheets would happen in the future warmer climate, we would like to know whether abrupt climate transitions would occur. Moreover, as suggested by ref. 14, the basic physical processes governing the response of the AMOC to the freshwater forcing in the North Atlantic under present-day or last glacial maximum conditions are essentially the same with a closed Bering Strait. Therefore, we judged that the present-day climate boundary condition would serve our purpose.

2. Significance of this study in comparison with other studies. ***a. A comparison of this study with EMIC-type studies.*** The purpose of this study is to address AMOC hysteresis, and to test the hypothesis of whether changes of sea level, especially the closure of the Bering Strait, can affect AMOC behavior. As indicated in the previous section, the initial freshwater forcing and the subsequent increment/decrement of this freshwater forcing are so slow in our simulations, it is sufficient to keep the AMOC in a quasiequilibrium state throughout our simulations. This feature also makes our simulations differ significantly from many previous freshwater hosing type simulations using coupled models (13, 14). What has been tested in those simulations is only the AMOC's response to a weak/strong (0.1 Sv/1 Sv) pulse of freshwater forcing in the subpolar North Atlantic which typically lasts only about 100 yrs. Afterwards this added freshwater is completely removed. Our simulations also differ from the AMOC hysteresis simulations using earth system models of intermediate complexity (EMICs). In the EMICs, many physical processes are simplified. For example, in Rahmstorf et al. (12), the EMICs use either a zonally averaged atmospheric model coupled to a zonally averaged ocean model, or a zonally averaged or an energy balance atmospheric model coupled to a coarse resolution ocean model (with a horizontal resolution of 3 degrees or more, and also a much coarser vertical resolution, such as 25 levels or less). Therefore, this type of model cannot simulate the full interactions among the air, sea, land, and sea ice systems, and the impact of the Bering Strait on the AMOC can, in general, not be properly simulated. The results from EMIC simulations, in general, agree qualitatively with AOGCMs under present-day or preindustrial climate conditions, such that a weaker/collapsed AMOC would induce a cooling effect in the North Atlantic. However, the magnitude of the temperature change in the North Atlantic is usually much weaker in the EMICs than in the AOGCMs (13).

b. The difference of our approach with previous studies. The idea that abrupt climate transitions can only occur during glacial times has been proposed before, e.g. ref. 15, 16, and they also suggested that the Bering Strait may have played a crucial role in these abrupt climate transitions. But in those studies, the proposed ideas are mostly speculation, not a solid demonstration. Here we put it into a more quantitative framework through a totally different approach—studying the role of the Bering Strait opening/closure on the AMOC hysteresis in a fully coupled, relatively high resolution state-of-the-art climate model. For example, the horizontal resolution in the CCSM3 ocean component is 1 degree latitude-longitude with finer resolution in the equatorial tropics and the subpolar North Atlantic. Therefore the effect of the Bering Strait on AMOC is more properly simulated in our model as demonstrated in a few previous studies (14, 16, 17). For example, the simulated Bering Strait throughflow is about 0.8 Sv in this version of the CCSM3 (Fig. S3), agreeing well with observations (18). Moreover, to more accurately test the Bering Strait's impact on AMOC hysteresis, our simulations are designed in such a way so that everything is identical in the two simulations except that in one the Bering Strait is open, and in the other the Bering Strait is closed. This mimics the sea level change during the last glacial period based on the reconstructed global sea level changes that suggest abrupt climate transitions occurred mostly when the global sea level was about 50 m below present-day level (Fig. 1). What we found here in our simulations is that the AMOC hysteresis, an important mechanism to explain the past abrupt climate transitions, only exists when the Bering Strait is closed. With an open Bering Strait, the AMOC hysteresis is almost nonexistent. Therefore, our results are fundamentally different from De Bore and Nof (15) although we both emphasized the importance of the Bering Strait closure. What's unique here is that we point out that if the AMOC hysteresis is a plausible mechanism to explain the past abrupt climate transitions, the closure/opening of the Bering Strait has fundamentally changed the AMOC hysteresis in such a way that makes abrupt climate transitions occur more frequently during glacial times when the Bering Strait is closed.

In addition, in our simulations we do not assume that the southern ocean winds are the primary driver of the AMOC as in De Bore and Nof (15, 19). As argued by De Bore and Nof (15, 19), the southern ocean winds push 4 Sv of southern ocean water into the Atlantic basin. With an active AMOC, this 4 Sv of southern ocean water will eventually flow southward as North Atlantic deep water. If the AMOC collapses, this 4 Sv of southern ocean water will flow out through the Bering Strait. As demonstrated previously (14, 16, 17) and also in Fig S4, the outflow at the Bering Strait when the AMOC collapses is only about 1 Sv, though we do have about 4 Sv of southern ocean water being pushed in the Atlantic. Therefore, the effect of the Bering Strait on dissipating the freshwater anomaly in the Atlantic might have been overestimated by De Bore and Nof (15, 19). On the other hand, the counterargument to De Bore and Nof (15) is that strong southern ocean winds also push southern ocean water into the Pacific and Indian Ocean basins. Should this water return to the southern ocean the same way as that pushed into the Atlantic via Bering Strait? Therefore, we speculate that the southern ocean winds may not be the main driver of the AMOC, although to some degree they do contribute to AMOC variations.

In summary, we propose here that the more fundamental causes of the unstable glacial climate and the more stable interglacial climate might rely on the ocean circulation's stability, since the discharge of large amounts of land-based ice occurred in both climates as suggested from reconstructed sea level changes (20) and other paleo proxy data (Fig. 1, ref. 21–25). If the AMOC has played a major role in the climate stability, the absence of AMOC hysteresis with an open Bering Strait and the existence of AMOC hysteresis with a closed Bering Strait might be the key insights to these climate differences.

c. Influence of the background mixing on AMOC hysteresis. A few previous studies indicate that AMOC hysteresis might only be an artifact of oceanic mixing coefficients (26–27). Using either an ocean general circulation model or an EMIC-type model, these studies, in general, found AMOC hysteresis when the oceanic background mixing coefficient was large enough. Otherwise AMOC hysteresis disappears. If these results were true for modern state-of-the-art climate models, it would not be possible to explain why, in our simulations, AMOC hysteresis exists only when the Bering Strait is closed. As stated in the previous section, in our simulations everything is identical except the Bering Strait, thus the background diffusivity is exactly the same in both simulations. Therefore, we suspect that the oceanic mixing coefficient might have played a role in AMOC hysteresis, especially in the earlier simple zonally averaged ocean models and the coarse resolution ocean general circulation models which can be run under a big range of diffusivity parameters. But this background diffusivity cannot determine the existence of AMOC hysteresis in modern state-of-the-art global coupled climate models, such as CCSM3.

In fact, in the ocean interior of CCSM3, the background internal wave mixing diffusivity (2) varies in the vertical from $0.1 \times 10^4\ m^2\,s^{-1}$ near the surface to $1.0 \times 10^4\ m^2\,s^{-1}$ in the abyss, and the transition occurs at about 1,000-m depth, which acts as a crude representation of the enhanced deep vertical mixing observed over rough topography (28). These values are unchanged when the model is used for simulations under different climate conditions, such as present-day conditions and last glacial maximum conditions. The choice of these mixing diffusivity coefficients cannot guarantee that a certain strength of the AMOC can be achieved when the ocean model is coupled with other components of the CCSM3, only that it will produce the simulated model climate in reasonable agreement with observations. Actually, the strength of the AMOC in CCSM3 is different from the AMOC in the ocean model standalone simulation forced by the best known observational surface data. This further suggests that the existence or not of AMOC hysteresis in our model is not determined by the diffusivity used here.

d. A comparison with the results of Liu et al. It is worth noting that the result from our closed Bering Strait simulation differs in some ways from the result of Liu et al. (29). First, two different versions of the CCSM3 are used. In the present study, a version of the CCSM3 with a T42 horizontal resolution atmospheric model and 1 degree horizontal resolution ocean model is used. In Liu et al.'s study, a version of the CCSM3 with a T31 horizontal resolution atmospheric model and 3 degree horizontal resolution ocean model was used. In addition, the vertical resolution of the ocean model is 40 levels in our simulation, but 25 levels in Liu et al.'s simulation. These differences produce a few important potentially different behaviors in the models. In the coarse resolution version (T31) of the CCSM3, the representation of the Bering Strait is not good, and deep convection in the North Atlantic is too weak, resulting in a 30% weaker AMOC in comparison to the T42 version of the model under present-day conditions (9). This weaker AMOC could be more sensitive to the external freshwater forcing.

Secondly, most of the freshwater forcing in Liu et al.'s simulation is added directly into the North Atlantic deep convection region between 50 and 70 °N, and part is added into the Gulf of Mexico. In our simulation, the freshwater forcing is added between 20 and 50 °N. More importantly, the initial freshwater forcing in Liu et al.'s simulation, however, is much larger (170 times) than that used in our simulation (0.0345 Sv vs. 0.0002 Sv). The increment/decrement later on is a similar magnitude as we used here or slightly smaller. Thus, it is quite possible that it is this large initial freshwater forcing that throws the AMOC out of the quasiequilibrium state, resulting in a linear slow down of the AMOC as freshwater forcing increases in Liu et al.'s simulation. After the AMOC collapses, the rate of the freshwater forcing decrement in Liu et al.'s simulation is about 50% of that in our simulation, and the AMOC stays in off mode for at least 800 yrs in Liu et al.'s simulation (Fig. S5 in their supporting online material). Then the AMOC restarts abruptly to produce the Błlling-Allerłd warming event. This more stable off mode, and the abrupt restart of the AMOC in Liu et al.'s simulation, may have produced the AMOC's hysteresis.

On the other hand, because our simulation with a closed Bering Strait is under the same climate boundary condition— the present-day condition, we cannot evaluate how much the glacial boundary condition would modify our results shown here. We speculate that our conclusions reached here would hold up at least qualitatively if the glacial boundary condition was used (see more detailed discussion in the next section). However, this speculation does need to be further investigated and the authors are planning to do so with a set of simulations the same as presented here except with glacial climate boundary conditions. These proposed simulations will take about two years to finish since we need to run each simulation for about 4,000 model years, and this is beyond the scope of the present study.

3. Discussions of the background climate. Although the present-day climate boundary condition is used in our experiments, we speculate that this would not significantly affect the application of our results to glacial conditions (note: here and in most of this paper, the glacial time period is defined as 80 to 11 thousand years before present [kyr BP], not the last glacial maximum which is about 21 kyr BP). This speculation is based on a previous study which suggests that the response of the AMOC to added freshwater forcing in the subpolar North Atlantic under present-day and last glacial maximum conditions is qualitatively the same when the Bering Strait is closed (14). In that study, the authors compared simulations with a closed Bering Strait under modern day climate conditions and last glacial maximum climate states. They found that the AMOC's response to a strong pulse of freshwater forcing (1 Sv for 100 yrs) in the subpolar North Atlantic is very similar in both cases regardless of their significantly different background climate. In contrast, the AMOC's response to freshwater forcing with an open Bering Strait under a modern day climate boundary condition is significantly different from those two simulations with a closed Bering Strait. They concluded that the effect of a closed Bering Strait to the divergence of an added freshwater anomaly in the subpolar North Atlantic is qualitatively the same under modern and last glacial maximum conditions.

Some previous studies using either ocean general circulation models or EMIC-type models suggest that AMOC hysteresis under glacial conditions differ from present-day conditions. For example, some indicate that although AMOC hysteresis was found in both climate conditions, the AMOC hysteresis cycle is narrower during glacial times than in present-day (30, 31) while others suggest that there are two stable modes of the AMOC under present day-conditions: (*i*) a warm conveyor belt (present-day AMOC) and (*ii*) an off mode. During glacial times, the evidence indicates that the AMOC had only one stable mode—the cold conveyor belt (32). However, the definition of the glacial conditions in these studies, in general, is the last glacial maximum around 21 thousand years ago. As shown in Fig. 1, most of the abrupt climate transitions did not occur during the last glacial maximum, but occurred instead during the time when the Bering Strait was just closed or nearly closed. This might indicate the climate conditions during the last glacial maximum could be different from other glacial times. One very important point which should be made is that in these models, due to the crudeness in model resolution, the Bering Strait is closed in both present-day and last glacial maximum conditions. Therefore, these simulations are more equivalent to our simulation with a closed Bering Strait. If the major difference of AMOC hysteresis between present-day and the last glacial maximum is the width of the hysteresis cycle, this would imply that our result with a closed Bering Strait would hold if glacial conditions were applied. If the last glacial AMOC hysteresis had indeed been a single stable state, we need to further test how stable it was with the AMOC in both active and off modes in our closed Bering Strait simulation. Preliminary tests show that the AMOC off mode with a closed Bering Strait seems more stable than the AMOC active mode. This suggests that conclusions from our closed Bering Strait simulation might hold for time periods when the glacial climate background was used, pending further investigation.

As we have mentioned in the main text, our results suggest that under modern climate conditions, the AMOC does not have hysteresis behavior. Therefore the AMOC would not collapse suddenly under greenhouse gas induced warming in the future, and consequently would not induce abrupt climate change. As suggested by model simulations (13, 14), a sudden shutdown of the AMOC in the future could occur under very strong freshwater forcing, such as a sudden collapse of the Greenland Ice Sheet. Up to now, it is very uncertain how the Greenland Ice Sheet would respond to greenhouse gas induced warming due to the lack of observations and the lack of understanding of ice sheet dynamics. A recent study (33) indicates that under idealized Greenland Ice Sheet melting scenarios, the AMOC could further weaken in comparison with the simulations which do not include the effect of Greenland Ice Sheet melting in the future. But indications are that the AMOC would not abruptly collapse.

As suggested from the paleoclimate record, the AMOC could have collapsed about 8,200 yrs before present (34) due to the disintegration of the ice dam and the draining of the ice sheet melt water from Lakes Agassiz and Ojibway, sending about 5 to 10 Sv of freshwater into the subpolar North Atlantic (35). Because the Bering Strait was open at that time, the freshwater anomaly in the North Atlantic was quickly transported out of the North Atlantic to the south and to the north. The part of the freshwater anomaly transported to the north was further transported into the North Pacific via the open Bering Strait as suggested by earlier studies (14, 16, 17). As a result, this abrupt climate change event is much shorter lived in comparison to those that occurred in the last glacial period.

Another way to view the effect of the opening of the Bering Strait at about 10.5 thousand years before present is that only one abrupt climate transition occurred at about 8.2 thousand years ago. However, the temperature changes in Greenland during this abrupt climate transition were less than half of those that occurred during those abrupt climate transitions in the last glacial period (36). Moreover, after the reopening of the Bering Strait due to the loss of land-based ice, the ice mass discharged into the ocean still amounted to about an equivalent 50-m global sea level rise. If the discharge of the land-based ice is the sole reason for the abrupt climate transitions, why did the abrupt climate transition not occur during the Holocene? Therefore, if the AMOC hysteresis was responsible for the past abrupt climate transitions during the glacial times, our simulations suggest that the AMOC hysteresis only exists when the Bering Strait is closed. With an open Bering Strait, the AMOC does not have hysteresis, thus it cannot induce abrupt climate transitions during the Holocene although significant discharge of land-based ice is still ongoing, especially during the first half of the Holocene. In other words, the discharge of the land-based ice into the North Atlantic might be only one of the necessary conditions for the occurrence of the abrupt climate transitions, with the AMOC hysteresis being another one. The lack of AMOC hysteresis due to the opening of the Bering Strait at about 10.5 thousand years before present leads to the stable Holocene climate.

4. The derivation of the relative sea level at Bering Strait. Eastern Siberia and Alaska both do not appear to have been extensively glaciated during either the last glacial cycle or MIS 6 (37–39). Therefore, the relative sea level change in the Bering Strait (Fig. 1) is predominantly controlled by the eustatic change and by the hydro-isostatic contributions from the changes in ocean volume and will not be strongly influenced by the assumptions made about the ice sheets. We confirmed this by converting the eustatic sea level (ESL) time series in Fig. 1 to relative sea level (RSL) using a mapping scheme derived from the ICE-5G/VM2 ice history-Earth model combination (40, 41). The full isostatic model has been used here, using the same theory, ice models and rheological parameters previously described in refs. 19 and 42, to predict the sea level change $\Delta\zeta(\varphi, t)$ as a function of location (φ) and time (t) and palaeo-bathymetry $h(\varphi, t) = h(\varphi, t0) - \Delta\zeta(\varphi, t)$ where $h(\varphi, t0)$ is the present-day topography. This present-day topography has been extracted from the bathymetric charts of the Admiralty Navigational Chart 4814 (43).

It is worth pointing out that the predicted RSL at the Bering Strait depends on the input ESL time series. Here we used the ESL time series of Lambeck and Chappell (19). The timing of the ESL minima in this time series agrees well with other independent ESL estimates, e.g. Siddall et al. (44).

1. Collins W-D, et al. (2006) The Community Climate System Model: CCSM3. *J Climate* 19:2122–2143.
2. Danabasoglu G, et al. (2006) Diurnal coupling in the tropical oceans of CCSM3. *J Climate* 19:2347–2365.
3. Smith R-D, Kortas S, Meltz B (1995) Curvilinear coordinates for global ocean models. *Los Alamos National Laboratory Tech. Rep.* LA-UR-95–1146, 38 pp.
4. Gent, P. R., J. C. McWilliams (1990) Isopycnal mixing in ocean circulation models. *J Phys Oceanogr* 20:150–155.
5. Large W-G, McWilliams J-C, Doney S-C (1994) Oceanic vertical mixing: A review and a model with a nonlocal boundary layer parameterization. *Rev Geophys* 32:363–403.
6. Meehl G-A, et al. (2006) Climate change projections for the twenty-first century and climate change commitment in the CCSM3. *J Climate* 19:2597–2616.
7. Ganachaud A, C Wunsch (2000) Improved estimates of global ocean circulation, heat transport and mixing from hydrographic data. *Nature* 408:453–457.
8. Pickard G-L, W-J Emery (1990) *Descriptive Physical Oceanography, An Introduction*. 5th Edition, Pergamon, Oxford.
9. Bryan F-O, et al. (2006) Response of the North Atlantic Thermohaline circulation and ventilation to increasing carbon dioxide in CCSM3. *J Climate* 19:2382–2397.
10. Otto-Bliesner B-L, E-C Brady (2010) The sensitivity of the climate response to the magnitude and location of freshwater forcing: last glacial maximum experiments. *Quaternary Sci Rev* 29:56–73.
11. Peltier W-R, Vettoretti G, Stastna M (2006) Atlantic meridional overturning and climate response to Arctic Ocean freshening. *Geophys Res Lett* 33:L06713, doi:10.1029/2005GL025251.

12. Rahmstorf S, et al. (2005) Thermohaline circulation hysteresis: A model intercomparison. *Geophys Res Lett* 32:L23605, doi:10.1029/2005GL023655.
13. Stouffer R-J, et al. (2006) Investigating the Causes of the response of the thermohaline circulation to past and future climate changes. *J Climate* 19:1365–1387.
14. Hu A, et al. (2008) Response of thermohaline circulation to freshwater forcing under present-day and LGM conditions. *J Climate* 21:2239–2258.
15. De Bore A-M, Nof D (2004) The Bering Strait's grip on the northern hemisphere climate. *Deep-Sea Res Pt 1* 51:1347–1366.
16. Hu A, Meehl G-A, Han W (2007) Role of the Bering Strait in the thermohaline circulation and abrupt climate change. *Geophys Res Lett* 34:L05704, doi:1029/2006GL028906.
17. Hu A, Meehl G-A (2005) Bering Strait throughflow and the thermohaline circulation. *Geophys Res Lett* 32:L24610, doi:10.1029/2005GL024424.
18. Woodgate R-A, Aagaard K (2005) Revising the Bering Strait freshwater flux into the Arctic Ocean. *Geophys Res Lett* 32:L02602, doi:10.1029/2004GL021747.
19. De Boer A-M, Nof D (2004) The exhaust valve of the North Atlantic. *J Climate* 17:417–422.
20. Lambeck K, Chappell J (2001) Sea level change through the last glacial cycle. *Science* 292:679–686.
21. North Greenland Ice Core Project members (2004) High-resolution record of Northern Hemisphere climate extending into the last interglacial period. *Nature* 431:147–151.
22. Dansgaard W, et al. (1993) Evidence for general instability for past climate from a 250-kyr ice-core record. *Nature* 364:218–220.
23. Ditlevsen P-D, Kristensen M-S, Andersen K-K (2005) The recurrence time of Dansgaard-Oeschger events and limits on the possible periodic component. *J Climate* 18:2594–2603.
24. Heinrich H (1988) Origin and consequences of cyclic ice rafting in the northeast Atlantic Ocean during the past 130,000 years. *Quat Res* 29:143–152.
25. Hemming S-R (2004) Heinrich events: Massive late Pleistocene detritus layers of the North Atlantic and their global climate imprint. *Rev Geophys* 42:RG1005, doi:10.1029/2003RG000128.
26. Prange M, Lohmann G, Paul A (2003) Influence of vertical mixing on the Thermohaline hysteresis: Analyses of an OGCM. *J Phys Oceanogr* 33:1707–1721.
27. Nof D, Van Gorder S, de Bore A (2007) Deos the Atlantic meridional overturning cell really have more than one stable steady state? *Deep-Sea Res Pt I* 54:2005–2021.
28. Ledwell J-R, et al. (2000) Evidence for enhanced mixing over rough topography in the abyssal ocean. *Nature* 403:179–182.
29. Liu Z, et al. (2009) Transient simulation of last deglaciation with a new mechanism for Bølling-Allerød warming. *Science* 325:310–314.
30. Prange M, Romanova V, Lohmann G (2002) The glacial Thermohaline circulation: Stable or unstable? *Geophys Res Lett* 29: doi:10.1029/2002GL015337.
31. Weber S-L, Drijfhout S-S (2007) Stability of the Atlantic meridional overturning circulation in the last glacial maximum climate. *Geophys Res Lett* 34:L22706, doi:10.1029/2007GL031437.
32. Ganopolski A, Rahmstorf S (2001) Rapid changes of glacial climate simulated in a coupled climate model. *Nature* 409:153–158.
33. Hu A, Meehl G-A, Han W, Yin J (2009) Transient response of the MOC and climate to potential melting of the Greenland Ice Sheet in the 21st century. *Geophys Res Lett* 36:L10707, doi:10.1029/2009GL037998.
34. Alley R-B, et al. (1997) Holocene climate instability: A prominent, widespread event 8200 yr ago. *Geology* 25:483–486.
35. Ellison C-R-W, Chapman M-R, Hall I-R (2006) Surface and deep ocean interactions during the cold climate event 8200 years ago. *Science* 312:1929–1932.
36. Alley R-B, et al. (2003) Abrupt climate change. *Science* 299:2005–2010.
37. Karhu J-A, et al. (2001) Constraints for the latest glacial advance on Wrangel Island, Arctic Ocean, from rock surface exposure dating. *Global Planet Change* 31:447–451.
38. Brigham-Grette J, et al. (2001) Last Interglacial (isotope stage 5) glacial and sea-level history of coastal Chukotka Peninsula and St. Lawrence Island, Western Beringia. *Quaternary Sci Rev* 20:419–436.
39. Kaufman D-S, Forman S-L, Lea P-D, Wobus C-W (1996) Age of pre-lat-Wisconsin glacial-estuarine sedimentation, Bristol Bay, Alaska. *Quaternary Res* 45:59–72.
40. Peltier W-R (2004) Global Glacial Isostasy and the Surface of the Ice-Age Earth: The ICE-5G (VM2) Model and GRACE, Invited Paper *Ann Rev Earth Pl Sc* 32:111–149.
41. Peltier W-R, Solheim L-P (2004) The climate of the Earth at Last Glacial Maximum: statistical equilibrium state and a mode of internal variability. *Quat Sci Rev.* 23:335–357.
42. Lambeck K, Purcell A, Funder S, Kjær K, Larsen E, Möller P (2006) Constraints on the Late Saalian to early Middle Weichselian ice sheet of Eurasia from field data and rebound modelling. *Boreas* 35:539–575.
43. Admiralty Navigational Chart 4814, Bering Sea—Northern Part, 1:3500000, UK Hydrographic Office, revised 1992.
44. Siddall M, et al. (2003) Sea-level fluctuations during the last glacial cycle. *Nature* 423:853–858.

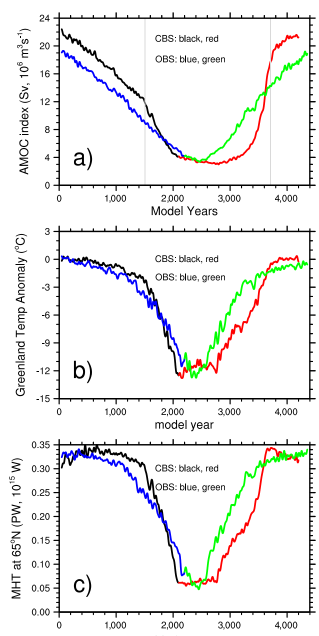

Fig. S1. The annual mean time series: the AMOC (*A*), Greenland surface temperature changes (*B*), and the oceanic meridional heat transport at 65 °N (*C*). The black, red lines are for the closed Bering Strait simulation, and blue, green lines for the open Bering Strait simulation. The black and blue lines represent the phase of freshwater forcing increase, and the red and green lines represent the phase of freshwater forcing decrease in these simulations.

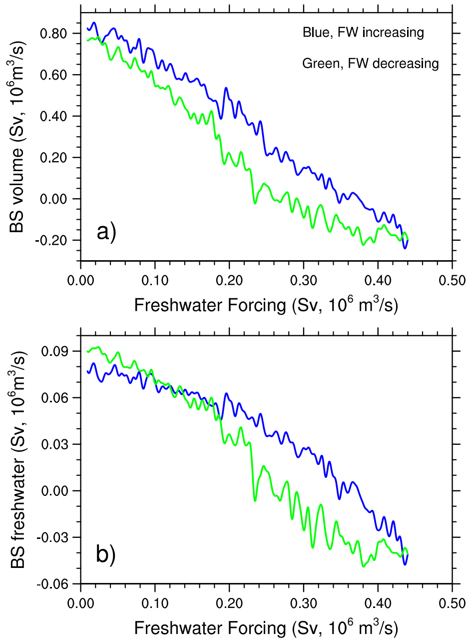

Fig. S2. The evolution of the Bering Strait throughflow (*A*) and the associated freshwater transport (*B*) in the open Bering Strait simulation with changes of the additional freshwater forcing. The blue line represents the phase of freshwater forcing increase, and the green line represents the phase of freshwater forcing decrease in these simulations.

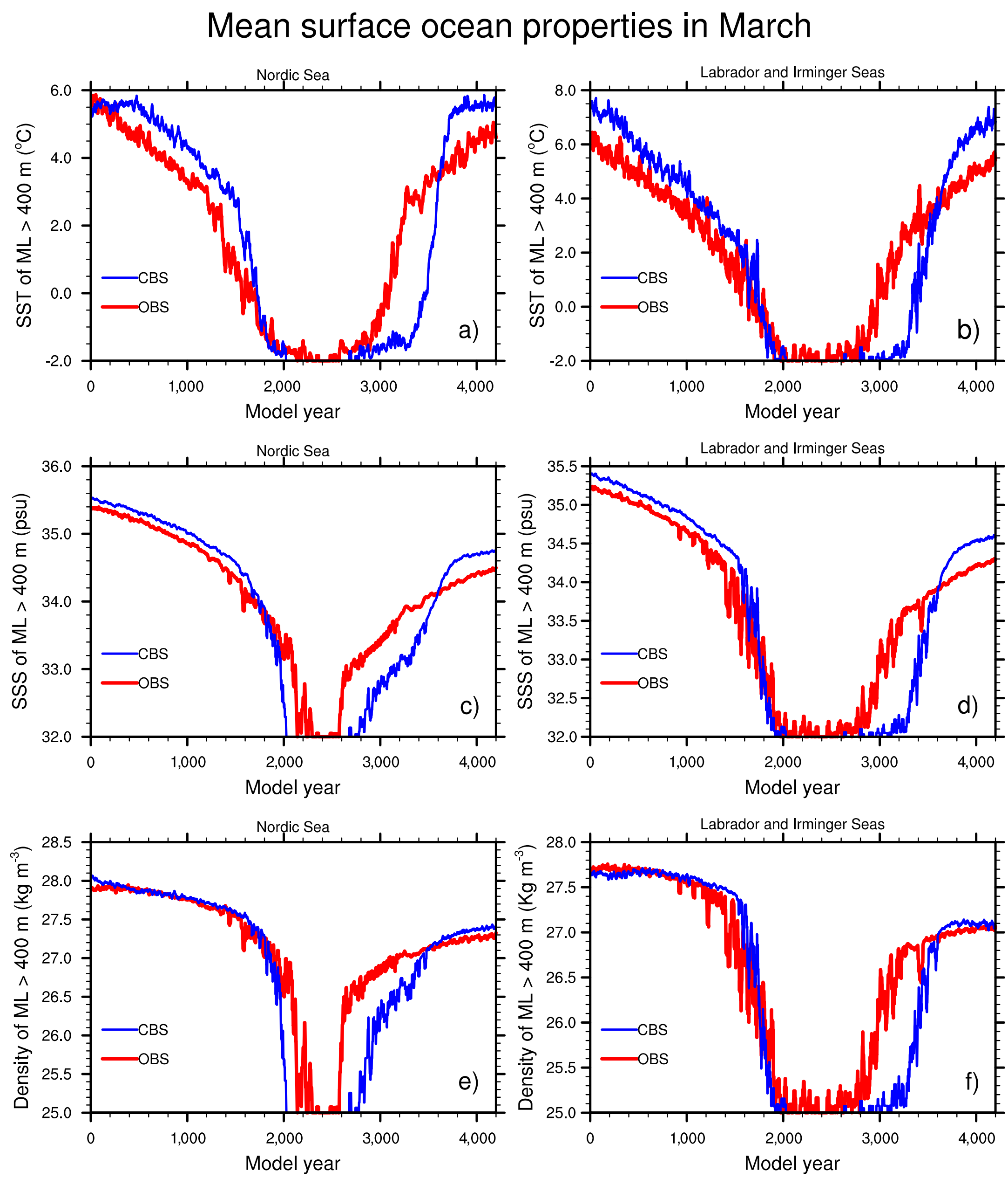

Fig. S3. The changes of the surface oceanic properties in the Nordic Sea (*Left*), and the Labrador and Irminger Seas (*Right*) for the regions where the March maximum mixed layer depth is deeper than 400 meters. Panels a and b are for the sea surface temperature (°C); panels c and d are for the sea surface salinity (psu); and panels e and f are for the surface potential density (kg/m^3). From this figure, it is clear that the changes of the surface density are primarily controlled by the changes of the sea surface salinity in our simulations. The contribution from surface temperature to surface potential density is small most of the time.

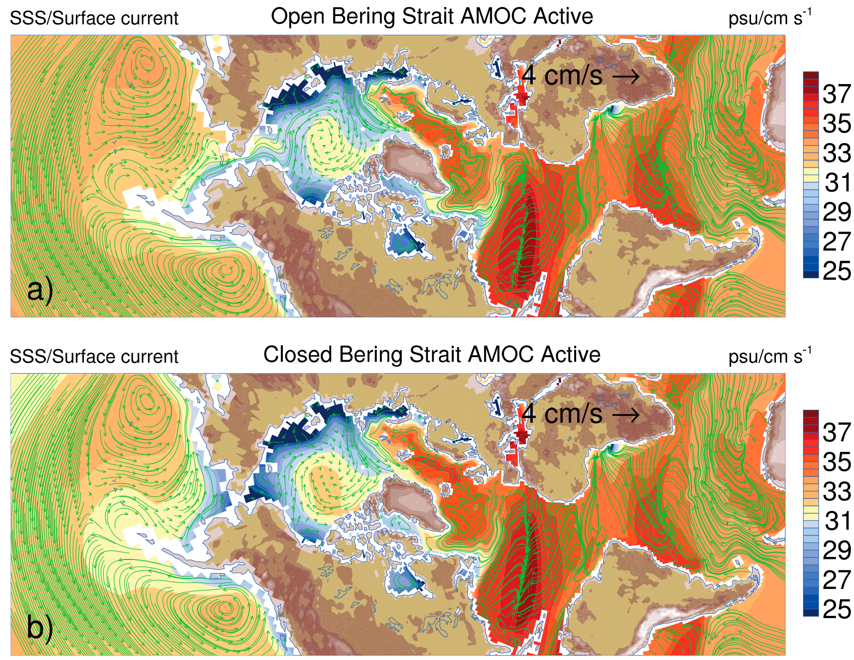

Fig. S4. Sea surface salinity (SSS) and sea surface currents when AMOC is "on" (control simulation) for the open Bering Strait (*A*) and closed Bering Strait (*B*) simulations. The arrows are the sea surface currents with units of cm/s. The shading is the SSS with a contour interval of 0.5 psu. In these simulations, no additional freshwater forcing is added to the North Atlantic.

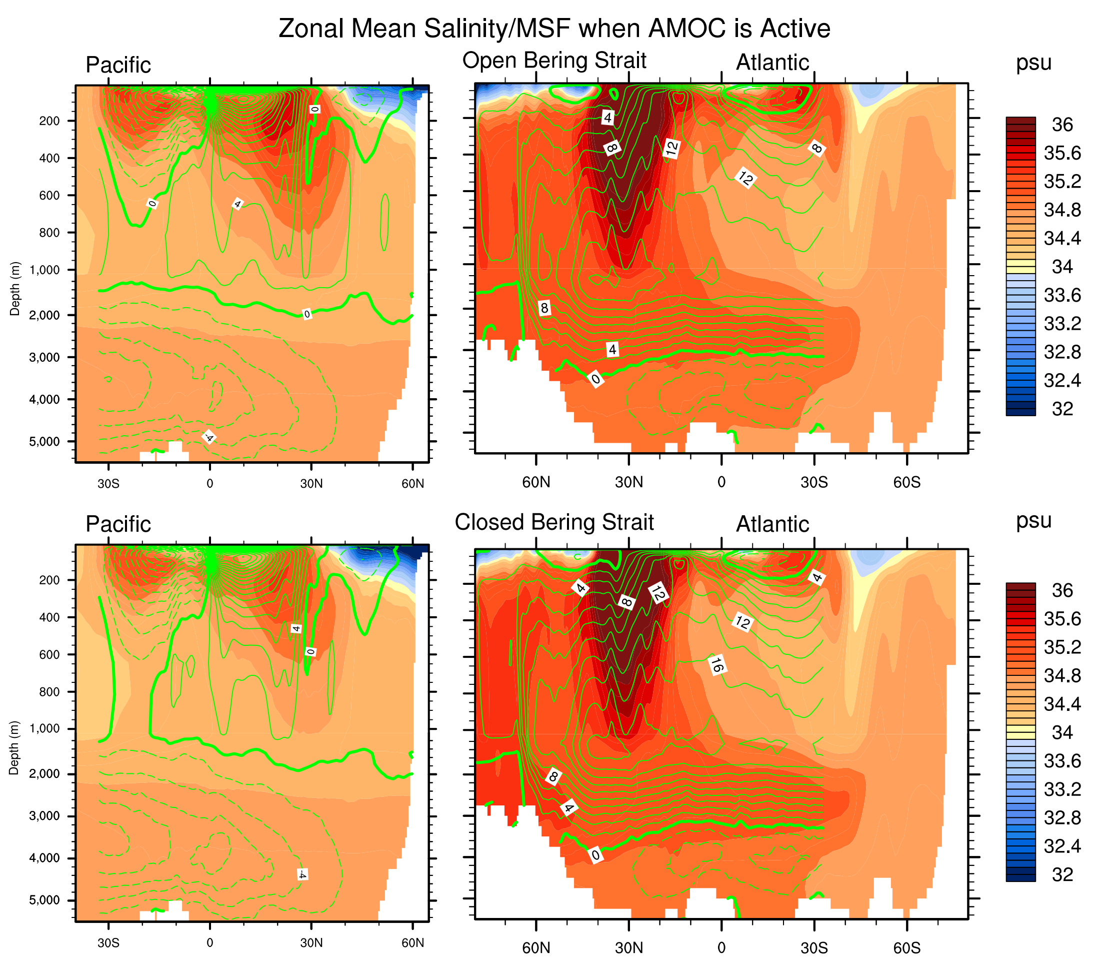

Fig. S5. Zonal mean salinity (shading) and meridional streamfunction (contour) in the Pacific (*Left*) and the Atlantic (*Right*) when AMOC is on. The contour interval of the meridional streamfunction is 2 Sv, and that of zonal mean salinity is 0.1 psu. The *Upper* are for the open Bering Strait simulation and *Lower* for the closed Bering Strait simulation. Note: the scale for the upper 1,000 meters of the ocean is stretched.

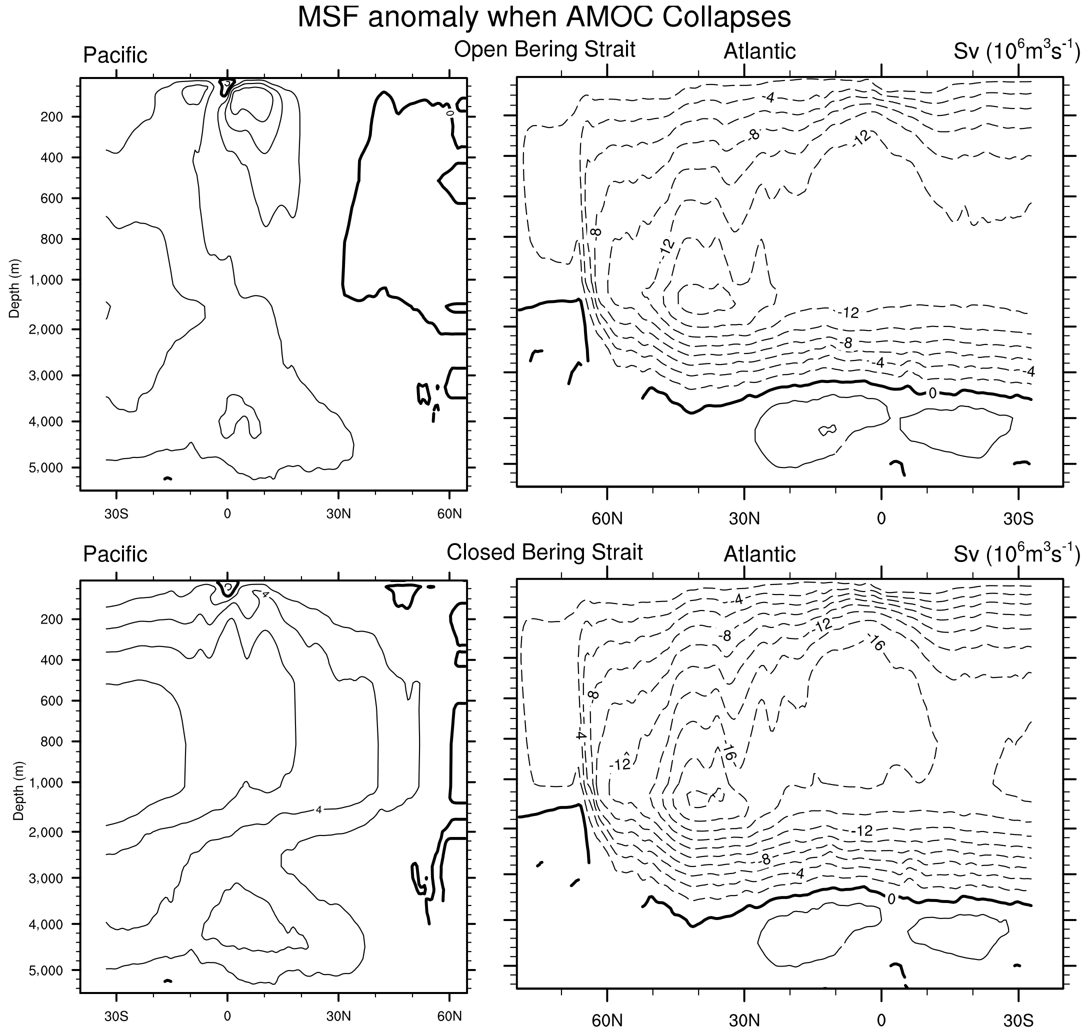

Fig. S6. The anomalous meridional streamfunction (MSF) in the Pacific and Atlantic when AMOC collapses relative to that when the AMOC is active. *Top* are the Pacific and Atlantic MSF for the open Bering Strait simulation, and the *Bottom* are the MSF for the closed Bering Strait simulation. The contour interval is 2 Sv.

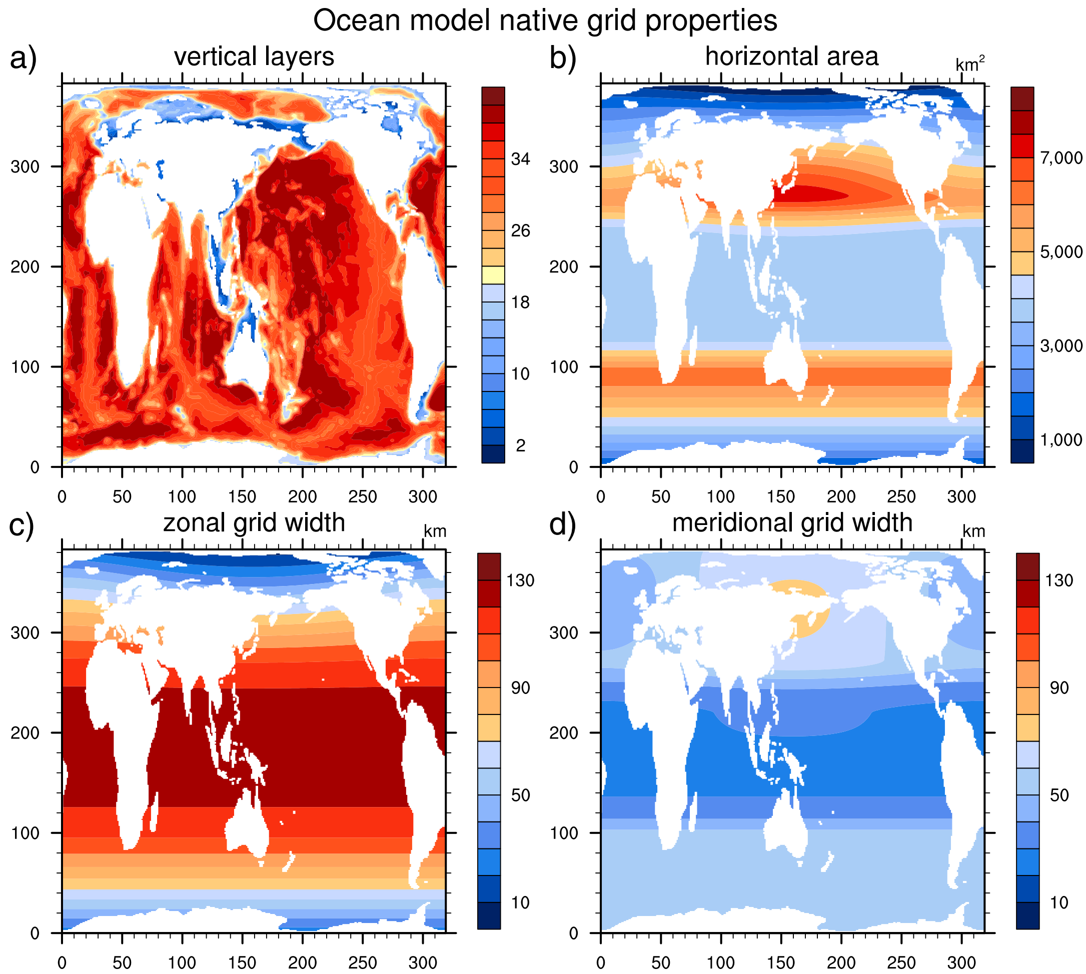

Fig. S7. The ocean model native grid properties. (*A*) is the number of layers at each ocean grid point which varies from 3 level to 40 levels; (*B*) is the cell area for each ocean grid point which varies from 545 km^2 to 7,289 km^2; (*C*) is the grid cell width in the zonal direction which varies from 8.6 km to 125 km; (*D*) is the grid cell width in the meridional direction which varies from 28.6 km to 72 km.